Solder Shape Design and Thermal Stress/Strain Analysis of Flip Chip Packaging Using Hybrid Method

Chang-Ming Liu[1](劉昌明)
E-Mail: d873776@oz.nthu.edu.tw

Kuo-Ning Chiang[2](江國寧)
Department of Power Mechanical Engineering
National Tsing Hua University
HsinChu, Taiwan 300, R.O.C.
E-Mail: knchiang@pme.nthu.edu.tw

Abstract

As the interconnection density of electronic packaging continues to increase, the fatigue-induced solder joint failure of surface mounted electronic devices become one of the most critical reliability themes in electronic packaging industry. Therefore, prediction of the shape of solder joint is a major event in the development of electronic packaging for its practical engineering application. In conventional electronic packaging, the geometrical dimensions of solder balls and solder pads still remain the same. The maximum thermally induced stress/strain occur on the top surface of each solder joint located farthest away the chip center may reduce the reliability life of entire packaging. In this research, a hybrid method combined with analytical and energy-based methods is utilized to predict force-balanced heights and geometry profiles of solder balls under various solder volume and pad dimensions as well as their relative location during the reflow process. Next, a finite element analysis code ANSYS is implemented to investigate the stress/strain behavior of solder balls in flip chip package under temperature cycles. The results reveal that as the flip chip package contains larger solder balls located at the corner area underneath the chip, the maximum equivalent plastic strain/stress is evidently reduced and the reliability cycles under thermal loading are enhanced. Furthermore, the results presented in this research can be used as a design guideline for area array interconnections such as CSP, flip chip, wafer level packaging and fine pitch BGA.

Introduction

Recently, a distinct trend in advanced electronic packaging technology is from BGA and CSP to flip chip and wafer level packaging technologies. The tendency to next generation technologies can enhance the performance of electronic packaging device such as high density I/O, better heat dissipation rate and tiny dimensions. As the density of electronic packaging continues to multiply, the fatigue-induced solder joint failure of area array type surface mounted electronic components has become one of the most significant topical subjects. In general, for the area array type packages, the failure phenomenon of the solder joint such as creep failure and crack are frequently resulted from the low cycle thermal fatigue. In addition, thermal strain and stress in solder joints under thermal loading are raised due to thermal expansion mismatch between the components of area array type packages such as substrate, solder balls, solder pads, silicon chip and solder mask. The thermally induced strain/stress existing in the interface between solder joints and silicon chip or between solder joints and solder pads may reduce the fatigue life and diminish the electric/thermal performance of the entire packages. Therefore, prediction of the surface profile and layout configuration of solder joint is critically needed in the development of electronic packaging for its practical engineering applications.

Several researches associated with the geometry / reliability prediction for area array type solder joints were proposed in the past decade. Charles et al.(1990) and Shah (1990) have demonstrated that the geometry profiles of the solder joints such as pad sizes, standoff heights and contact angles had great influence on the fatigue life of the solder balls during temperature cycle [1-2]. Chiang (1998) and Heinrich et al. (1993) have developed prediction models for area array type solder joints on the basis of analytical algorithm [3-4]. On the other hand, Chiang (1998), Patra et al. (1995) and Brakke (1999) constructed other prediction models for solder balls on the strength of energy-based method [5-7]. Moreover, Chiang (1999) presented a novel approach named hybrid method combined analytical algorithm and energy-based method to predict the static force-balanced surface profiles and restoring forces of solder joints in multiple/hybrid pad shapes (HPS) area array packages under reflow process [8]. In addition, Yeh et al. (1996) investigated the influence of several key factors such as temperature shock effects, underfill thickness, die thickness, PWB thickness, solder joint location, die size, underfill fillet profile, initial PWB warpage, material properties on the reliability analysis of flip chip with underfill [9]. However, few researches were proposed to elucidate the impact of pad sizes and solder volume as well as their layout on the thermally induced strain/stress behavior and reliability cycles of solder joints in no-underfill flip chip package (Figure 1).

---

[1] Graduate Assistant
[2] Associate Professor

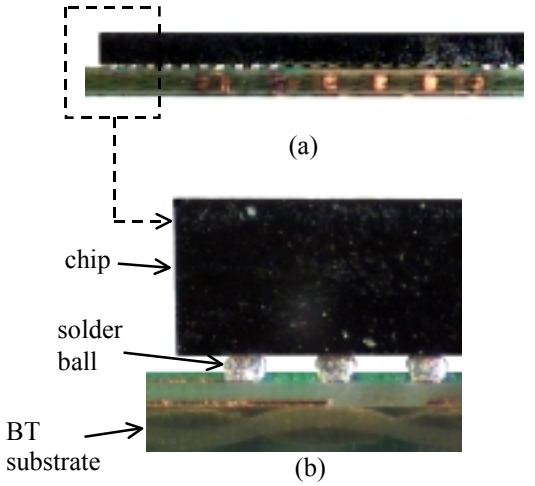

Figure 1: Cross-section view of no-underfill flip-chip package

Hybrid Method for Multiple Ball System

Energy-based method

An energy based program named Surface Evolver is implemented to estimate the surface profiles and restoring force of molten solder balls. For the liquid solder joint of BGA type packages, the surface tension energy is more important than the gravitational force. The surface tension is defined as the force per unit length of liquid surface which is tangential to the edge of the surface and tends to minimize the surface area of the liquid. The Surface Evolver can simulate the liquid surface by dismember an initial simplex surface into a set of triangular facets and then iterate these facets towards a minimal energy situation using conjugate gradient method. In the static equilibrium situation, the total energy of the molten solder contains three major origins: surface tension, gravitation and pressure,

$$E = \iint_S T dA + \iiint_V G\rho z dV - PV \qquad (1)$$

where T is the surface tension of the free surface, A is the area of a facet, ρ is the density of solder joint, G is the acceleration due to gravity, z is the height of a facet, P is the net pressure in the molten solder, and V is the volume of solder joint. From the divergence theorem, the second term of the energy E can be express as:

$$\iiint_V G\rho z dV = \iint_S \rho G \frac{z^2}{2} \vec{k} \bullet d\vec{A} \qquad (2)$$

where $\vec{k}$ is the unit vector along the gravitational force. Equation (1) can be rewritten as:

$$E = \iint_S T dA + \iint_S \rho G \frac{z^2}{2} \vec{k} \bullet d\vec{A} - PV \qquad (3)$$

Given a perturbation function $\vec{p} = (z + ZH)\vec{j}/2ZH$, which leaves the bottom plane fixed and gives a unit shift to the top plane. The unconstrained variation of the energy is

$$\begin{aligned} \delta E = {} & T \iint_S (\mathrm{div}\, \vec{p} - \vec{N} \bullet D\vec{p} \bullet \vec{N}) dA \\ & + \rho G \iint_S \left(\mathrm{div}\left(\frac{z^2}{2}\vec{k}\right)\vec{p} - \mathrm{curl}\left(\vec{p} \times \frac{z^2}{2}\vec{k}\right) \right) \bullet d\vec{A} \\ & - P \iint_S \vec{p} \bullet d\vec{A} \end{aligned} \qquad (4)$$

where $\vec{N}$ is the unit normal vector of a facet. It is significant to work with piecewise linear surfaces that the perturbations be likewise piecewise linear. Therefore, the force of the molten solder is

$$\begin{aligned} F = {} & T \iint_S -\frac{N_z N_y}{2ZH} dA + \rho G \iint_S -\frac{z^2}{4ZH} \vec{k} \bullet d\vec{A} \\ & - P \iint_S \frac{z + ZH}{2ZH} \vec{j} \bullet d\vec{A} \end{aligned} \qquad (5)$$

where $\vec{j}$ is the unit vector along the second axis of the reference coordinate, ZH is the 1/2 height of solder ball. In the above equations, the objective of perturbation function is to provide a displacement on the upper or lower pads of solder joint. Next, the energy difference from equilibrium of the perturbed system is derived by calculus of variation and the force can be obtained. Different perturbations on solder pads will produce distinct geometry profile and restoring force of molten solder joints. From the viewpoint of reliability, higher standoff height and smaller contact angle are preferred. Therefore, solder volume and pad dimension as well as their relative location have be arranged with optimal design.

Analytical method

Several assumptions are to be followed to predict the geometry profile of molten solder balls for round pads (Figure 2):

1.The molten solder ball is in static equilibrium when the solder solidifies.

2.The solder pads on the chip and substrate are circular and are perfectly aligned when the solder solidifies.

3.The surface profile of the molten solder ball is axially-symmetric.

4.The meridian defining the free surface of the solder joint is assumed to be a circular arc.

5.The solder pads are completely covered by the solder, but the solder does not spread beyond the pads.

6.The solder pad is assumed to be perfectly wettable, while the surrounding solder resist material is perfectly non-wettable.

7.The volumetric shrinkage due to solder solidification can be neglected.

8.For multiple ball model, the array of solder joints has a doubly-symmetric layout, i.e., the array possesses two

orthogonal planes of symmetry (Figure 3).

9.The center of gravity of the component is aligned with the center of the array (Figure 3).

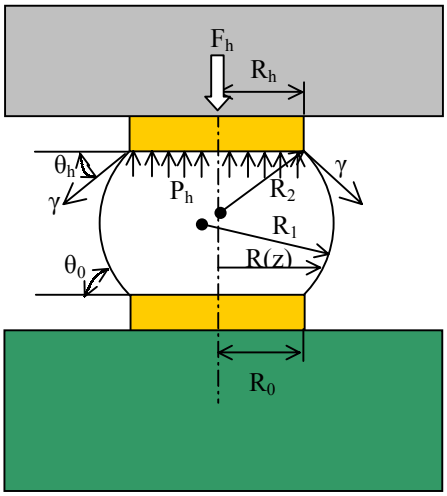

Figure 2: Free body diagram of solder ball with axial-symmetric round pads.

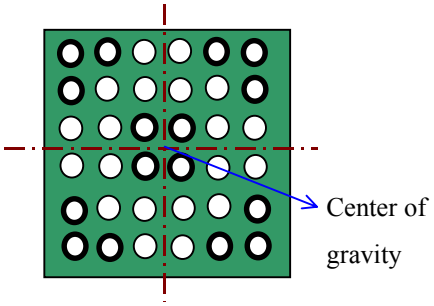

Figure 3: One example of doubly symmetric array layout.

The surface profile of solder ball is calculated by Laplace-Young equation. The governing equation of molten solder joint under static equilibrium is expressed as

$$P_0 = P_a + \gamma\left(\frac{1}{R_1} + \frac{1}{R_2}\right) + \rho g(h - z) \qquad (6)$$

where P_a , P_0 , γ, ρ , g, and z are the ambient pressure, internal pressure, surface tension, density of solder, acceleration of gravity and the height of a certain point on the solder surface, respectively, and R_1 and R_2 are the principal radii of curvature of solder surface at height h. In equation (6), the variables P, R, R_1 , R_2 , are functions of z (P=P(z); R=R(z); $R_1=R_1(z)$; $R_2=R_2(z)$). In the molten solder joint, the gravitational force is much less than the surface tension. Therefore, the third term in equation (6) can be neglected and the governing equation can be rewritten as:

$$P = P_0 - P_a = \gamma\left(\frac{1}{R_1} + \frac{1}{R_2}\right) \qquad (7)$$

The principle radii of curvature of the solder surface R_1, R_2 can be derived according to the third assumption:

$$P = \gamma\left\{-\frac{R''}{\left[1+(R')^2\right]^{3/2}} + \frac{1}{R\sqrt{1+(R')^2}}\right\} \qquad (8)$$

From Figure 2, the equation of static equilibrium is expressed as:

$$F_h + \left[\gamma\sin(\pi - \theta_h)\right]\cdot 2\pi R - P_h \pi R_h^{\,2} = 0 \qquad (9)$$

where F_h represents the weight of components or the force applied at upper solder pads and this force can be balanced by internal pressure and surface tension of solder joint. Moreover, the volume constraint of solder joint with an unknown standoff height h is expressed as:

$$V = \pi\int_0^h [R(z)]^2\,dz \qquad (10)$$

The unbalanced force for a single molten solder ball is expressed as:

$$\delta F = F_h - \frac{\pi R_h}{2hR}\left[\mp(R_0 + R_h) - \sqrt{\frac{4R^2h^2}{(R_0+R_h)^2 + h^2}} - h^2\right] \qquad (11)$$

According to equation (11), an initial value of standoff height h should be assigned to iterate the unbalanced force. However, increasing or decreasing the standoff height h to iterate the loop of solution procedure is required if the solder ball system is not in the static equilibrium. The force balanced standoff height and final geometry profile of the molten solder ball is obtained once the forces exerted on the system are balanced with each other.

The single ball model (SBM) described in the previous section can be incorporated into the multiple ball model (MBM) by iterating on the height h of the array until the sum of all joint reaction forces on the component balances the component weight W:

$$W - \sum_{i=1}^{n} F^{(i)} = 0 \qquad (12)$$

where n is the total number of joints in the array and superscript i denotes a quantity associated with the ith joint. Component weight is considered positive when the component is attached to the upper side of the solder ball during a standard reflow operation. A negative weight is specified when the component is hanging from the lower surface of the substrate. The initial value of standoff height h_{min} is defined as the smallest height based on the geometry limitation. The value of h is increased in the MBM until the system achieves static equilibrium. Input parameters to the MBM are the component weight,

number of solder joints, dimensions of solder pads, surface tensions, and solder volumes for each joint in the array. Output parameters include the restoring force of individual solder joint and geometry data.

Hybrid method

In this research, a hybrid method including analytical and energy-based methods are employed to predict static force-balanced heights, geometry profiles and restoring forces of solder balls under various solder volume and pad dimensions as well as their relative location during the reflow process. The hybrid pad shapes system studied in this research contains two kinds of pad sizes with two kinds of solder volume, and benchmark models are demonstrated in Figures 4(b) to Fig4(e). The larger solder pad and solder balls are placed at the central area and corner area underneath the chip to reduce the maximum strain/stress of solder balls that located at corner area. These layout configurations of solder balls can increase standoff height and enhance the thermal/mechanical performance of flip chip packaging.

Once the solder ball layout is determined, the hybrid method can be employed to calculate the force-balanced standoff heights and to produce surface profiles of these round-pad-shape solder balls. For the hybrid method, simulation of the round-pad-shape solder ball in multiple ball models is based on analytical algorithm. The analytical algorithm can provide accurate results with short period if the shape of solder pad remains round and the volume of the solder ball is small enough to neglect the gravitational effect. Next, the output result from analytical method is considered as the input parameters for energy-based method which takes gravitational force into account to modify the restoring force and geometry data. The key points of solder surface can also be obtained using curve fitting program and be imported into commercial finite element code ANSYS to construct finite element model for advanced thermo-mechanical/reliability analysis. The accumulative equivalent plastic strain during the three cycles and equivalent plastic strain increment within each cycle are calculated to investigate the influence of pad sizes, solder volume and relative locations on the maximum strain/stress of the solder balls at the corner area underneath the silicon chip. Moreover, the equivalent plastic strain increment $\Delta \varepsilon_p$ within the last cycle is put into Coffin-Manson equation (equation (13)) to predict the reliability cycles of solder balls under temperature cycling. The preliminary results reveal that as the no-underfill flip chip contains one large ball at the corner area underneath the chip farthest away the chip center, the maximum equivalent plastic strain is obviously reduced over conventional electronic packaging.

$$N_f = 0.4405\left(\Delta\varepsilon_p\right)^{-1.96} \qquad (13)$$

Therefore, larger solder balls and solder pads at the corner area could enhance the reliability cycles and structural stiffness of the entire electronic device.

Applications and Discussion

In this research, five no-underfill flip chip packages are presented to investigate the influence of solder pad size and solder ball volume on the strain/stress behavior of these packages. These five models are schematically displayed in Figure 4.

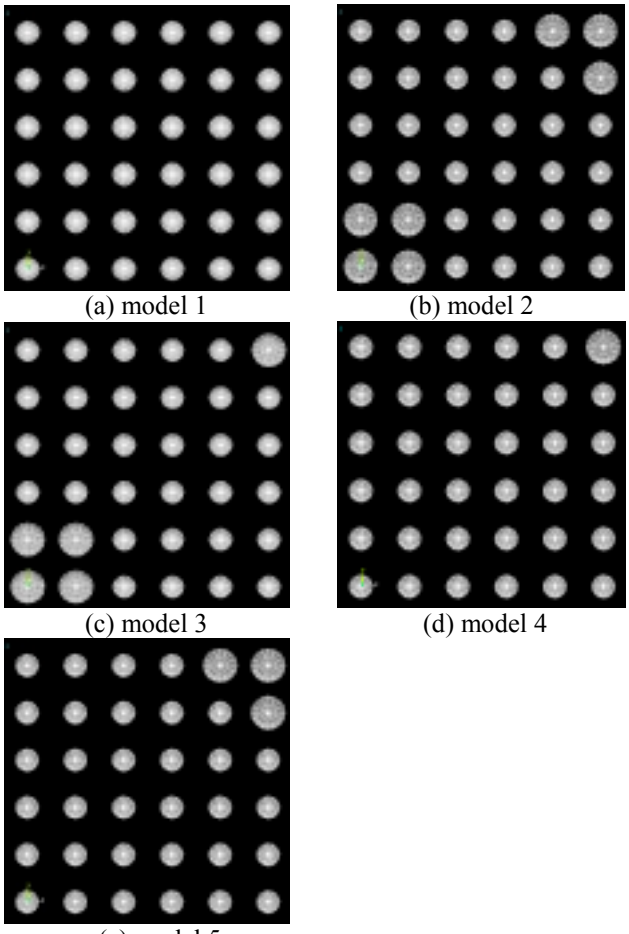

(a) model 1 (b) model 2

(c) model 3 (d) model 4

(e) model 5

Figure 4: 3D quarter models of five no-underfill flip chip packages (The center of each model is located at lower-left corner of each Figure).

The thermally induced stress/strain properties of the five models are investigated using 3D quarter finite element models performed in ANSYS software. The boundary condition and oblique view of the model are illustrated in Figure 5. The size of the die is 9.6mm X 9.6mm X 0.35mm and the size of the substrate is 25mm X 25mm X 0.5mm. The pad sizes and solder volume are listed in table 1. Model 1 is the conventional area array structure, which the pad size and solder volume remain equivalent. The other four models contain two different pad sizes and solder volume. The results of the four HPS/MBM models will be compared with the conventional package (model 1) to validate the pad size and volume effect. The detailed information of the five models is listed in table 2. The linear and temperature dependent material properties are given in table 3 and Figure 6. The material of solder joint used in this research is assumed to be eutectic solder (63% Sn / 37% Pb) and is perfectly wettable to the

copper pads. The analysis steps of temperature loading are described as follows:

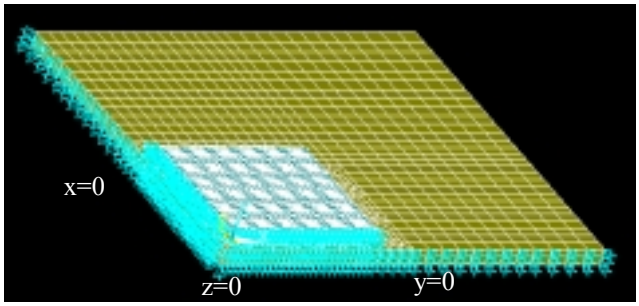

Figure 5: The boundary conditions of these five models.

Table 1: Pads sizes and solder volumes

Pad	Diameter(mm)	Solder volume(mm^3)
Small ball (R1)	0.250	0.030
Large ball(R2)	0.400	0.069

Table 2: Detailed information of the five models.

Model	Large ball number (location)	Quarter package weight (g)
Model 1	0	0.51
Model 2	7 (4 at center; 3 at corner)	0.51
Model 3	5 (4 at center; 1 at corner)	0.51
Model 4	1 (1 corner)	0.51
Model 5	3 (3 corner)	0.51

Table 3: Linear material properties of each component.

Material Properties	Young's modulus (MPa)	CTE(ppm/℃)	Poisson's Ratio
Die	112400	2.62	0.28
Solder ball	17177.8	23.9	0.35
FR4 substrate	18200	16	0.19

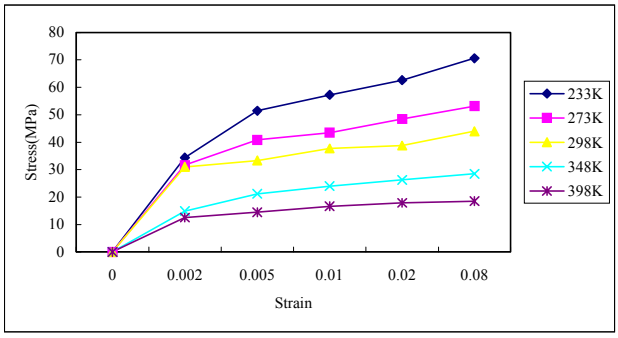

Figure 6: Temperature dependent stress/strain curve of eutectic solder ball.

Step 0. These five models are assumed to be stress free at 298K.

Step 1. Increase the temperature to 398K in 7.5 minutes.

Step 2. Hold the package at 398K for 15minutes.

Step 3. Decrease the temperature to 233K in 15 minutes.

Step 4. Hold the package at 233K for 15 minutes.

Step 5. Increase the temperature to 298K in 7.5 minutes.

Step 6. Repeat steps 1 to 5 for two more cycles to get a stable increment equivalent plastic strain.

The results of this research include standoff heights, contact angles, maximum equivalent plastic strain of solder balls and stress distribution of silicon dice.

This research calculates the geometry/shape results of the five models. The hybrid method predicts the standoff heights of the HPS/MBM system and the geometry information of each ball in short period. This geometry / shape information is very useful with finite element reliability analysis. The system standoff heights and contact angle are tabulated in table 4. Normally, the higher standoff height with blunter contact angle provides better reliability life cycles for solder ball. The hybrid method demonstrates a rapid and practical manner to predict the solder reflow shapes of area array packages. Moreover, the geometry/shape information can be transferred to FEM software for advanced reliability analyses.

Table 4: Some typical geometry data of five HPS/MBM models

Models	System standoff height (mm)	Contact angles(degree)	
		Small ball	Large ball
Model 1	0.3019	142.2	-
Model 2	0.3224	135.7	146.6
Model 3	0.3154	136.2	148.2
Model 4	0.3046	138.3	154.4
Model 5	0.3100	137.1	151.2

The main purpose of this research is to investigate the influence of pad size and solder volume on strain/stress behavior of solder ball. The number assignment of each corner ball is shown in Figure 7. The increment of maximum equivalent plastic strain of the five models in each cycle is displayed in Figures 8 to 12. From these Figures, it is clear that the incremental equivalent plastic strain already becomes stable at cycle 3. Therefore, it is reasonable to use the incremental equivalent plastic strain at cycle 3 as the input for Coffin-Manson equation (equation (13)). Furthermore, the strain in ball number 2 or 3 is evidently lower than that in ball number 1 by about 21%. Table 5 lists the decreasing percentage of maximum accumulative plastic equivalent stain at the end of temperature cycle 3 in ball number 2 or 3 to that in ball number 1. Therefore, if ball number 1 performs as structural dummy ball, the strain of ball number 2 or 3 in model 3 will provide the superior performance, which reduces the strain by approximately 35.69%. Table 6 and Figure 13 summarize the maximum incremental equivalent plastic strain in the four corner balls at the end of temperature cycle 3 for the five benchmark models.

The fatigue life cycles of solder balls are predicted using empirical Coffin-Manson equation (equation (13)) and the results are plotted in Figure 14. Figures 13 and 14 reveal that model 2 has the best strain result for ball number 1, however, model 3 will have the best strain result for ball number 2 or 3.

Furthermore, the maximum normal stress of silicon die along three axial direction is located in the interface between die and solder ball number 1. In these five models, the absolute value of the maximum normal stress of dice is less than 50MPa. Therefore, the possibility of die cracking could be neglected.

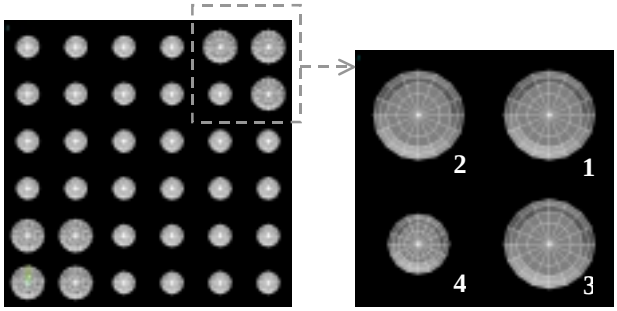

Figure 7: The number of each corner balls.

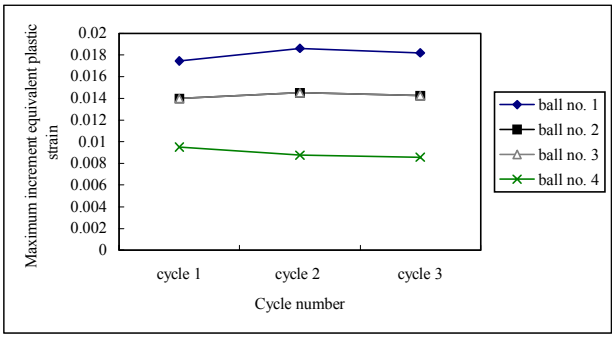

Figure 8: Increment of maximum equivalent plastic strain of model 1 in each cycle.

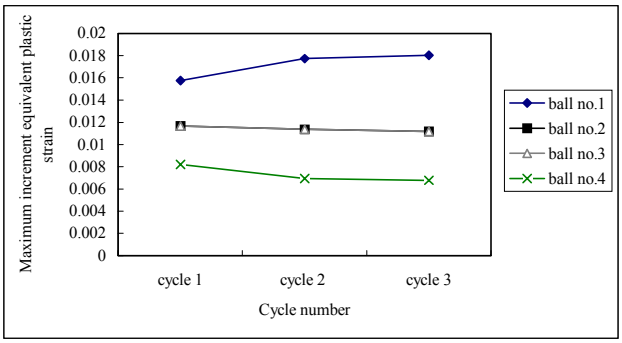

Figure 9: Increment of maximum equivalent plastic strain of model 4 in each cycle.

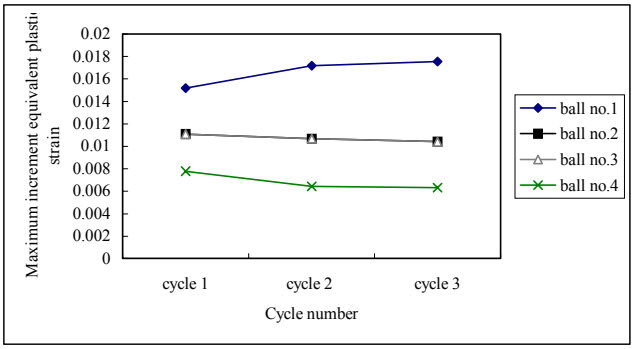

Figure 10: Increment of maximum equivalent plastic strain of model 3 in each cycle.

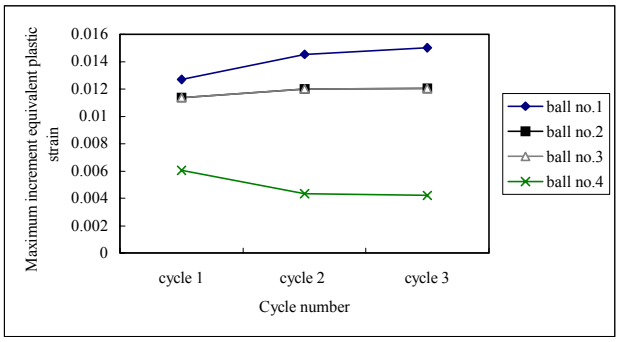

Figure 11: Increment of maximum equivalent plastic strain of model 5 in each cycle.

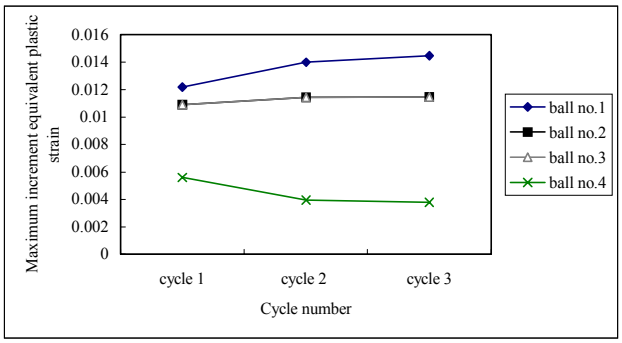

Figure 12: Increment of maximum equivalent plastic strain of model 2 in each cycle.

Table 5: Decreasing percentage of maximum accumulative equivalent plastic strain in ball number 2 and 3 to that in ball number 1.

	Model 1	Model 2	Model 3	Model 4	Model 5
%	21.26	16.90	35.69	33.68	16.1

Table 6: Maximum accumulative equivalent plastic strain in the four corner balls. (t = cycle 3)

Model	Model 1 (0)	model 4 (1)	model 3 (5)	model 5 (3)	model 2 (7)
large ball location		0 center; 1 corner	4 center; 1 corner	0 center; 3 corner	4 center; 3 corner
ball no. 1	0.05425	0.05151	0.04996	0.04221	0.04062
ball no. 2 and 3	0.04272	0.03416	0.03214	0.03541	0.03376
ball no. 4	0.02685	0.02192	0.02052	0.01460	0.01331

Conclusions

This research employs hybrid method for solder reflow shape prediction and finite element method to investigate the effect of pad sizes and solder volume as well as their relative location on the stress/strain behavior of solder joints and silicon die. This hybrid method can effectively calculate the standoff height of HPS/MBM system and other geometry/shape information such as contact angle. Generally, the higher standoff height with blunter contact angle will provide better reliability cycles of solder ball. In this research, five models are constructed

to evaluate the pad size and solder volume effect on the

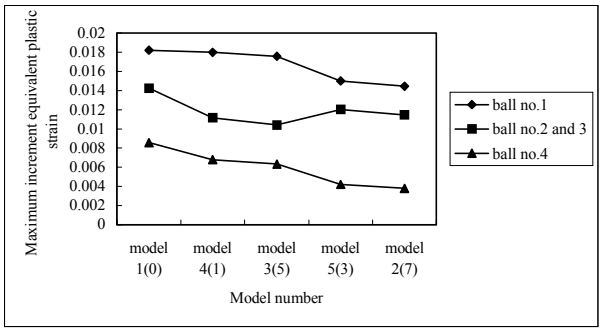

Figure 13: Maximum incremental equivalent plastic strain in the four corner balls. (t = cycle 3)

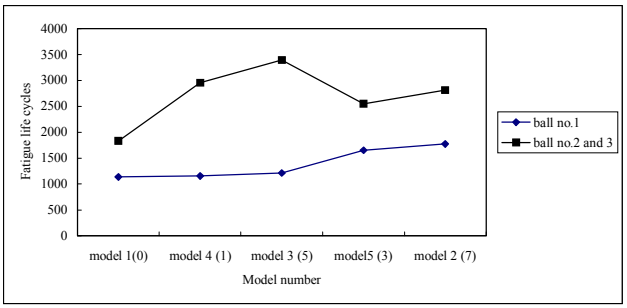

Figure 14: Fatigue life cycles of solder balls.

equivalent plastic strain of solder joints and normal stress of silicon die. The maximum equivalent plastic strain of solder balls is found to be located in the top surface of solder ball number 1. These results summarize that model 2 have preferable reliability performance for the solder ball number 1. However, model 3 have the best reliability cycles of solder ball number 2 or 3 as the ball number 1 is used to be structural dummy ball. Furthermore, the results obtained in this research could be used as design guidelines for flip chip, ultra CSP and wafer level packages with various pad sizes, solder volume and layout configurations. The optimal design for HPS/MBM packages with the hybrid method could fulfill the requirement of long-period reliability.

Acknowledgments

The authors would like to thank the National Science Council for supplying this research (project NSC 89-2212-E-007-081).

References

1. Charles, H. K., and Clatterbaugh, G. V., "Solder Joint Reliability – Design Implications from Finite Element Modeling and Experimental Testing, " *ASME Journal of Electronic Packaging*, Vol. 112, No.2, 1990, pp.135-146.
2. Shah, M. K., "Analysis of Parameters Influencing Stress in the Solder Joint of Leadless Chip Capacitors, " *ASME Journal of Electronic Packaging*, Vol.118, No.3, 1990, pp.122-126.
3. Chiang, K. N., and Chen, W. L., "Electronic Packaging Reflow Shape Prediction for the Solder Mask Defined Ball Grid Array," *ASME Journal of Electronic Packaging*, Vol.120, 1998, pp.175-178.
4. Heinrich, S. M., Liedtke, P.E., Nigro, N.J., Elkouh, A. F., and Lee, P.S., "Effect of Chip and Pad Geometry on Solder Joint Formation in SMT," *Journal of Electronic Packaging*, Vol. 115, 1993, pp.433-439.
5. Chiang, K.N., Cheng, H.C., "On Enhancing Eutectic Solder Joint Reliability Using A 2nd Reflow Process Approach," *ASME Winter Annual Meeting*, Thermo-Mechanical Characterization of Evolving Packaging Materials and Structures Symposium, EEP-Vol. 24, pp.21-25, Nov. 15-20, 1998, Anaheim, CA, USA
6. Patra, S. K., Sritharan, S. S., and Lee, Y. C., "Quantitative Characterization of a Flip-Chip Solder Joint," Journal of Applied Mechanics, Vol. 62, 1995, pp.390-397.
7. Brakke, K. A., *Surface Evolver Manual*, Version 2.14, The Geometry Center, 1300 S. Second St., Minneapolis, MN 55454, 1999.
8. Chiang, K. N., Cheng, H. C., Liu, C. M., "A Comparison of Thermal Stress/Strain Behavior of Ellipse/Round Solder Pads," 1999InterPACK, EEP-Vol.26-1, 1999, pp.413-418, *Advances in Electronic Packaging ASME*, Hawaii, U.S.A.
9. Yeh, C. P., Zhou, W. X., and Wyatt, K., "Parametric Finite Element Analysis of Flip Chip Reliability," *The International Journal of Microcircuits and Electronic Packaging*, Vol.19, Number 2, Second Quarter 1996, pp.120-127.